Final manuscript Corrosion Science 90 (2015) 1-4

Direct observation of hydrogen and deuterium in oxide grain boundaries in corroded Zirconium alloys

G. Sundell[1], M. Thuvander[1], A.K. Yatim[2], H. Nordin[3], H.-O. Andrén[1]

E-mail: gustav.sundell@chalmers.se
Phone: +46-(0)31-772 3291

[1] Dept. of Applied Physics
Chalmers University of Technology
412 96 Göteborg, Sweden

[2] I. Institute of Physics (IA)
RWTH Aachen University
52056 Aachen, Germany

[3] Atomic Energy of Canada Ltd
Chalk River Laboratories
Chalk River Ontario
K0J 1J0 Canada

Abstract

Atom probe tomography has been used to the study the distribution of hydrogen and deuterium in the oxide scale of two common zirconium alloys after autoclave testing in H_2O and D_2O, respectively. Comparison between hydrogen and deuterium in the mass spectra allows for separation of hydrogen as a corrosion product from adsorbed H_2 gas from the vacuum chamber. Enrichment of hydrogen and deuterium, as OH^+ and OD^+, was observed in grain boundaries. The grain boundaries were identified through segregation of iron. This lends experimental support to existing theories for the mechanism of hydrogen pick-up in zirconium alloys.

Keywords: A. Atom probe; B. Hydrogen pick-up; C. Zirconium alloys; D. Corrosion; E. Grain boundaries; F. Deuterium

Introduction

Perhaps the least understood degradation phenomenon of zirconium alloys for nuclear applications is the mechanism of hydrogen pick-up. During waterside corrosion, a fraction of the hydrogen that is released in the water decomposition reaction will be absorbed by the fuel cladding [1] and precipitate as hydrides, eventually leading to embrittlement of the material [2]. Although many studies have been conducted on the subject, no widely accepted mechanism exists that describe how hydrogen penetrates the passive ZrO_2 films that are formed on the alloys. Various routes for hydrogen ingress have been proposed, such as interstitial diffusion through the ZrO_2 lattice [3], migration through crystallite

boundaries in the oxide [4], fast transport through secondary phase particles (SPPs) in the oxide scale [5] and H_2O propagation through microcracks in the passive film [6]. The inherent volatility of hydrogen renders experimental validation of such hypotheses problematic.

Atom probe tomography has some unique virtues for hydrogen detection, such as near-atomic resolution and equal sensitivity to all elements in the periodic table. A major drawback is that substantial amounts of hydrogen from the analysis chamber adsorbs onto the specimen during experiments, obscuring the true hydrogen content in the analyzed material [7]. However, studies have shown that this obstacle may be overcome by using samples exposed to deuterium [8-13]. Deuterium-containing ions in the APT mass spectra shift the peaks by 1 Da with respect to the hydrogen-containing ions that result from the adsorbed gas.

In this study, we use atom probe tomography to compare the hydrogen-deuterium distribution in the oxide scale of two common zirconium-based cladding materials – one used in boiling light water reactors (BWR) and another used in CANDU heavy water reactors. Specifically, this allows for spatial mapping of hydroxide/deuterium oxide ions in the spectra that we link to the hydrogen ingress through the passive oxide films.

Materials and experimental details

The BWR material used in this study is a Zircaloy-2 tube of the Westinghouse designated LK3™ heat treatment scheme (see [14] for details). The material is alloyed with 1.32% Sn, 0.17% Fe, 0.10% Cr and 0.05% Ni (all in wt%). The material was corroded in H_2O in a static steam autoclave at 400°C and 10.3 MPa for 15 days, producing an average oxide thickness of 2.3 µm.

The CANDU material is a Zr-2.5Nb tube that was subjected to 12% cold drawing after extrusion at 815°C. The material is alloyed with 2.5% Nb and contains 0.114% Fe and 0.083 % C (all in wt%). The sample was corroded in a heavy water autoclave operated at 335°C for 150 days to produce an average oxide thickness of 2.8 µm. LiOH was added to the autoclave water, raising the pH_a to 10.5.

Needle-shaped atom probe specimens were prepared using a combined focused ion beam and scanning electron microscope workstation (FIB-SEM) in a conventional lift-out procedure followed by a tip-sharpening step with annular milling [15]. The geometry of the tips were such that the direction of the analyses runs normal to the metal-oxide interface, and therefore parallel to the columnar oxide grains that are formed during waterside oxidation of zirconium alloys [16]. The probed volumes in this study are located in the middle of the so-called barrier oxide, approximately 500 nm away from the metal-oxide interface.

The Zircaloy-2 samples were analyzed in an Imago LEAP 3000X HR atom probe system. Field evaporation is initiated by laser pulsing with green light (λ = 532 nm) at a 200 kHz pulse rate, using 0.5 nJ pulse energy. The temperature of the

tips was held at 70 K and the pressure in the chamber was approximately 10^{-9} Pa. The Zr-2.5Nb samples were analyzed in a Cameca LEAP 4000X Si system. Field evaporation was in this case initiated by laser pulsing with UV light (λ = 355 nm) at a 200 kHz pulse rate, using 0.1 nJ pulse energy. The temperature of the tips was held at 40 K and the pressure in the chamber was approximately 10^{-9} Pa. APT data was analyzed using the IVAS 3.6.6 software. The reconstructions were made using the default k-factor of 3.3 and an evaporation field of 28 V/nm.

Results

H_2O-corroded samples

A number of different peaks in the spectra from the ZrO_2 phase can be identified as hydrogen-containing ions, with the most abundant being H^+, H_2^+ and OH^+, with small amounts of H_3^+ and H_2O^+ present. The H^+, H_2^+, H_3^+ and the H_2O^+ ions, at 1, 2, 3 and 18 Da respectively, are distributed homogeneously in the 3D reconstructions (see Figure 1). The OH^+ peak at 17 Da, on the other hand, is in some analyses enriched along planar features in the oxide scale. Although APT does not give explicit crystallographic information, we can take advantage of the fact that Fe is found in oxide crystallite boundaries [17], so that oxide grain boundaries can readily be identified. Interestingly, the OH^+ peak clearly co-localizes with the Fe^{2+} peak at 28 Da along grain boundary planes in the oxide scale. There is noticeably a correlation between the OH^+ ions and the Fe-infused grain boundary in the oxide, and an enrichment of OH^+ ions in the boundary is evident. However, grain boundaries can be low-field areas of the APT specimen [18], which may attract elevated gas adsorption quantities from the chamber that will field evaporate together with an adjacent oxygen atom. Therefore, the OH^+ peak in H_2O-corroded samples cannot unequivocally be attributed to hydrogen originating from the corrosion process. Furthermore, additional contribution to the signal from oxygen from the material combining with adsorbed hydrogen species may dilute the apparent localization of the peak.

D_2O-corroded samples

Similar to the Zircaloy-2 samples, Fe is detected in oxide grain boundaries also in the Zr-2.5Nb alloy, thus enabling identification of boundaries in the oxide also in this material. The H^+, H_2^+ and the H_3^+ are homogenously distributed in the reconstructions (see Figure 2). However, in the beginning of the analysis a focus alignment of the laser beam with respect to the tip was performed. This results in enhanced adsorption of gas from the vacuum, which is reflected in the two horizontal planes with elevated H^+, H_2^+ and H_3^+ levels at the top of the analysis. In the D_2O-corroded materials we can categorically dismiss the entire signal at 1 Da and 17 Da as adsorbed species from the vacuum chamber, as no H was present during the autoclave corrosion process. By extension, other hydrogen-containing species that exhibit similar spatial distributions as H^+ can also be ascribed to gas from the vacuum chamber. Therefore, the elevated 3 Da signal during the laser scan is a strong indication that the peak results from adsorbed H_3^+ species and not a combined DH^+ ion.

Strikingly, the peak that is localized to Fe-decorated grain boundaries is now found at 18 Da in the mass spectra of the D_2O-corroded samples. The OH^+ peak is instead homogeneously distributed in the 3D reconstructions and has no discernable correlation with the grain boundary. As the peak at 18 Da does not co-localize with the 17 Da peak at all, it clearly distinguishes itself from the confirmed adsorbate-containing OH^+ species. A small peak at 18 Da without spatial localization is found also in the H_2O-corroded material, indicating that the non-localized part of the OD signal is partly adsorbed H_2O species.

Discussion

We can for the first time show direct evidence of hydrogen and deuterium enrichment in oxide grain boundaries in autoclave-tested zirconium alloys. This lends experimental support to the hydrogen pick-up mechanism of migration along oxide grain boundaries, which has been proposed by other authors [4, 19]. It should be noted that although hydrogen and deuterium are detected in the form of OH or OD, it is not possible to draw any conclusions regarding their chemical or molecular state in the oxide. On the other hand, fourier transformed infrared raman spectroscopy (FTIR) studies by Ramasubramanian et al. have suggested that hydroxyls and hydrogen-bonded water are indeed present in the oxide [4], indicating that this is the chemical environment of the hydrogen in the grain boundaries. As the barrier oxide typically consists of nano-crystalline columnar grains, any random APT analysis will likely capture a number of grain boundaries. Not all APT analyses from the oxide contain hydrogen-enriched boundaries and it is therefore reasonable to assume that only a fraction of these boundaries act as hydrogen transport paths.

These results imply that the texture and the grain boundary chemistry of the oxide must be taken into account when designing zirconium alloys with the view to mitigate hydrogen pick-up. Texture and grain structure of the barrier oxide layer have been identified as important factors for oxidation and hydrogen pick-up previously [20, 21], and may to some degree be controlled in the processing of cladding tubes. The grain boundary chemistry may influence the electrochemical properties of the oxide scale by moving the cathodic half-cell reaction of the corrosion process away from the metal-oxide interface [22].

Conclusions

Hydrogen and deuterium are found to be enriched in oxide grain boundaries of autoclave-tested zirconium alloys. Hydrogen originating from the corrosion process can be separated from adsorbed residual H_2 gas from the vacuum chamber by comparing mass spectra from H_2O and D_2O corroded alloys. Although the electrochemical state of the detected hydrogen species could not be determined, the results give an indication that oxide grain boundaries are pathways for hydrogen pick-up in zirconium alloys.

Acknowledgements

The authors would like to thank the MUZIC-2 consortium for helpful discussions. Westinghouse Electric Sweden AB, Sandvik Materials Technology AB, Vattenfall

AB, the Swedish Research Council and the Deutsch Forschungsgesellschaft (funding within SFB 917) are gratefully acknowledged for their financial support.

References

[1] S. Kass, J. Electrochem. Soc. 107 (1960) 594-597
[2] C.E. Coleman, D. Hardie, J. Less-Common Metals 11 (1966) 168-85
[3] T. Smith, J. Nucl. Mat. 18 (1966) 323-336
[4] N. Ramasubramanian, V. Perovic, M. Leger, Zirconium in the Nuclear Industry: 12th International Symposium, ASTM STP 1354, 2000, 853-876
[5] Y. Hatano, M. Sugisaki, K. Kitano, M. Hayashi, Zirconium in the Nuclear Industry: 12th International Symposium, ASTM STP 1354, 2000, 901-917
[6] B. Cox, J. Nucl. Mat. 264 (1999) 283-294
[7] G. Sundell, M. Thuvander, H.-O. Andrén, Ultramicroscopy 132 (2013) 285-289
[8] G.L. Kellogg, J.K.G. Panitz, Appl. Phys. Lett. 37 (1980) 625-627
[9] J. A. Spitznagel, S.S. Brenner, M.K. Miller, W.J. Choyke, J. Nucl. Mat. 122-123 (1984) 252-253
[10] Y. Ishikawa, T. Yoshimura, J. Vacuum Soc. Jpn., 41 (1998) 210-212
[11] R. Gemma, T. Al-Kassab, R. Kirchheim, A. Pundt, Scr. Mat. 67 (2012) 903-906
[12] H. Takamizawa, K. Hoshi, Y. Shimizu, F. Yano, K. Inoue, S. Nagata, T. Shikama, Y. Nagai, Appl. Phys. Express 6 (2013)
[13] D. Haley, S.V. Merzlikin, P. Choi, D. Raabe, Int. J. Hydrogen Energy039 (2014) 12221-12229
[14] T. Andersson, T. Thorvaldsson, A. Wilson, A.M. Wardle, Improvements in Water Reactor Fuel Technology and Utilization, IAEA, Vienna, Austria, (1987), 435-449
[15] D.J. Larson, D.T. Ford, A.K. Petford-Long, H. Liew, M.G. Blamire, A. Cerezo, G.D.W. Smith, Ultramicroscopy 79 (1999), 287-293
[16] S. Nanikawa, Y. Etoh, S. Shimada, T. Kubo, K. Ito, H. Harada, Zirconium in the Nuclear Industry: 12th International Symposium, ASTM STP 1354, 2000, 815-835
[17] G. Sundell, M. Thuvander, H.-O. Andrén, Corr. Sci. 65 (2012) 10-12
[18] M. Thuvander, H.–O. Andrén, Mater. Character. 44 (2000) 87-100
[19] M. Lindgren, I. Panas, RSC Adv. 3 (2013) 21613-21619
[20] N. Ni, D. Hudson, J. Wei, P. Wang, S. Lozano-Perez, G.D.W. Smith, J.M. Sykes, S.S. Yardley, K.L. Moore, S. Lyon, R. Cottis, M. Preuss,
C.R.M. Grovenor, Acta Mater. 60 (2012) 7132-7149
[21] K. Une, K. Sakamoto, M. Aomi, J. Matsunaga, Y. Etoh, I. Takagi, S. Miyamura, T. Kobayashi, K. Ito, Zirconium in the Nuclear Industry: 16th International Symposium, ASTM STP 1529, 2012, 401-432
[22] M. Lindgren, I. Panas, G. Sundell, L. Hallstadius M. Thuvander, H.-O. Andrén, Zirconium in the Nuclear Industry 17th International Symposium, ASTM STP (2013), *In Press*

Figures

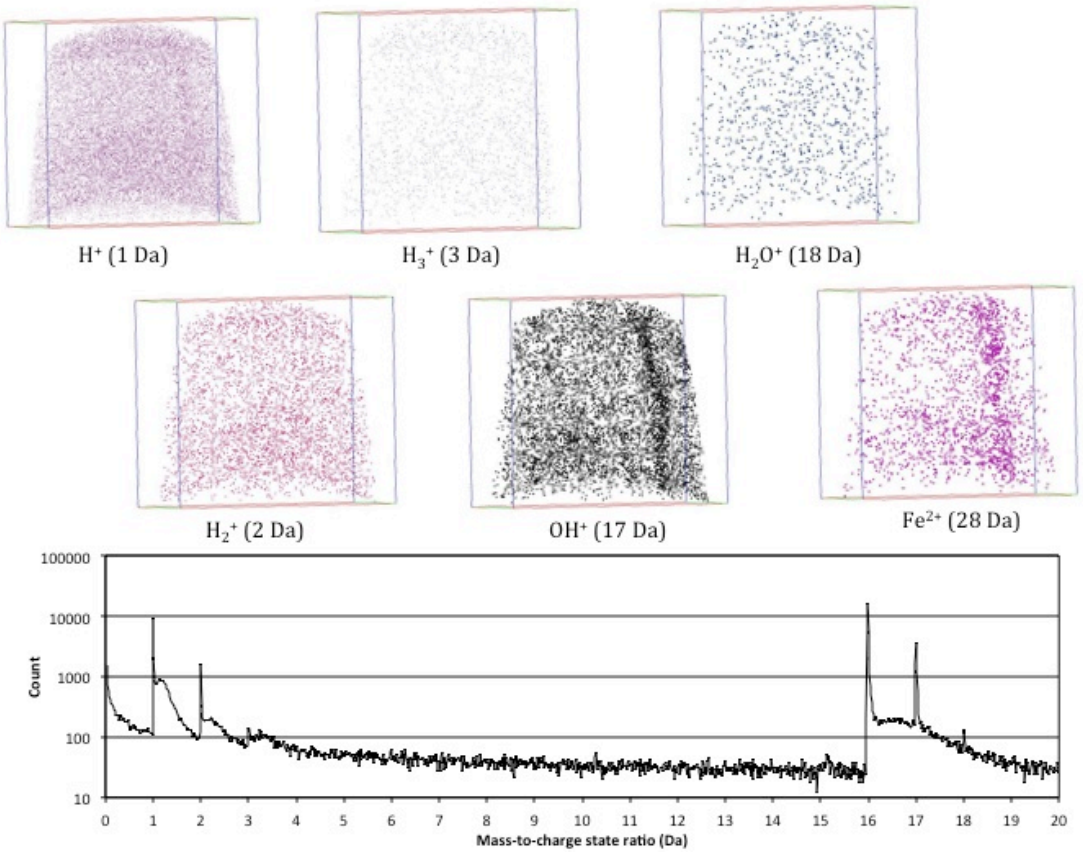

Figure 1: Mass spectrum and 3D reconstructions showing the spatial distribution of the dominant hydrogen-containing peaks from the oxide of Zircaloy-2. Note the enrichment of OH and Fe along a grain boundary. The size of the boxes in the reconstruction is 70x70x70 nm³.

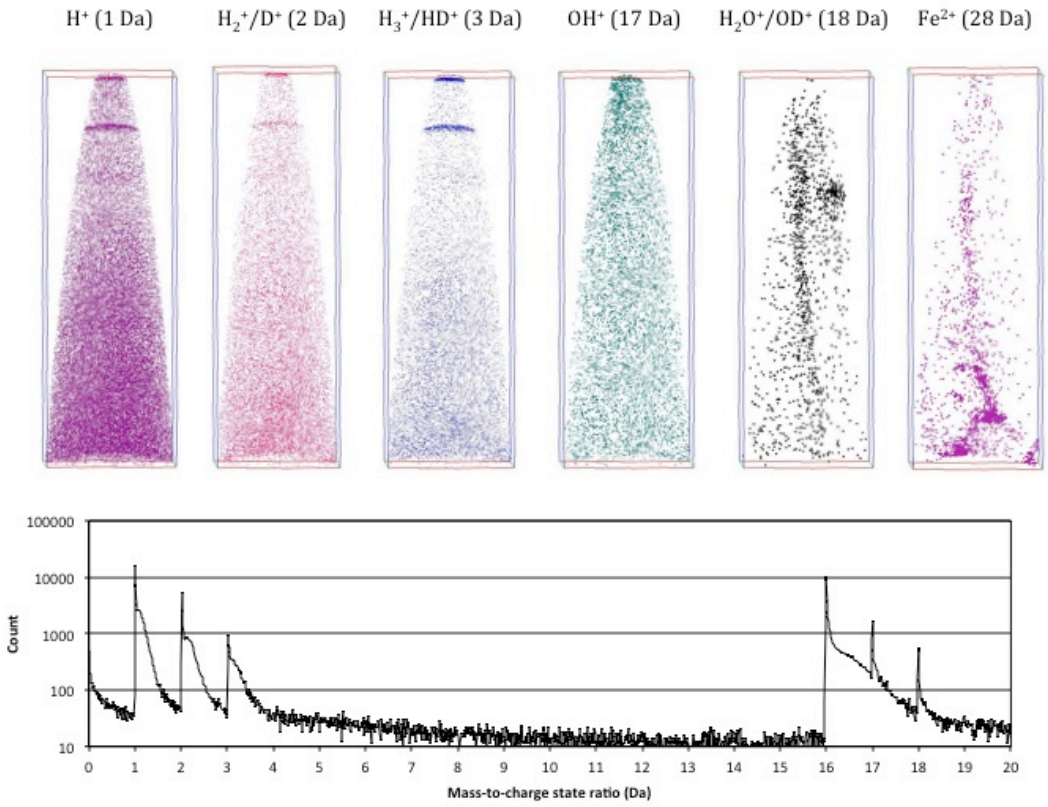

Figure 2: Mass spectrum and 3D reconstructions showing the spatial distribution of the dominant hydrogen-containing peaks from the oxide of Zr-2.5Nb. Note the enrichment of OD and Fe along a grain boundary. The horizontal enrichment of H, H_2 and H_3 is adsorbate species resulting from a laser alignment scan. The size of the boxes in the reconstruction is 190x65x65 nm^3.